

Cycloheptyl-fused *N,N,N'*-chromium catalysts with selectivity for vinyl-terminated polyethylene waxes: thermal optimization and polymer functionalization

Received 00th January 20xx,
Accepted 00th January 20xx

DOI: 10.1039/x0xx00000x

www.rsc.org/

Chuanbing Huang,^{a,b} Yongfeng Huang,^{a,c} Yanping Ma,^a Gregory A. Solan,^{*,a,d} Yang Sun,^a Xinquan Hu^{*,c} and Wen-Hua Sun^{*,a,b}

Five chromium(III) chloride complexes, [2-((Ar)N=CMe)-9-(N(Ar))C₁₀H₁₀N]CrCl₃ (Ar = 2,6-Me₂C₆H₃ **Cr1**, 2,6-Et₂C₆H₃ **Cr2**, 2,6-*i*-Pr₂C₆H₃ **Cr3**, 2,4,6-Me₃C₆H₂ **Cr4**, 2,6-Et₂-4-MeC₆H₂ **Cr5**), each chelated by a sterically and electronically different cycloheptyl-fused *N,N,N'*-bis(imino)pyridine, have been synthesized by the reactions of CrCl₃(THF)₃ with the corresponding ligand (**L1/L1'** – **L5/L5'**). The molecular structure of **Cr2** highlights both the steric properties exerted by the inequivalent *N*-2,6-ethylphenyl groups and the puckering of the fused cycloheptyl ring; a distorted octahedral geometry is conferred about the metal center. On activation with methylaluminoxane (MAO) or modified MAO (MMAO), **Cr1** – **Cr5** displayed their optimal activity for ethylene polymerization at temperatures between 70 and 80 °C with the least sterically demanding **Cr1** proving the most productive (1.44 × 10⁷ g (PE) mol⁻¹ (Cr) h⁻¹). The polyethylenes formed are of low molecular weight (*M_w* range: 0.66 – 3.56 kg mol⁻¹) with narrow molecular weight distributions and display high levels of end-group unsaturation. Furthermore, the amenability of these vinyl-terminated polyethylenes to undergo functionalization via epoxidation has been demonstrated.

Introduction

Motivated by the discovery that 2,6-bis(imino)pyridine-iron and cobalt complexes can catalyze the polymerization of ethylene to form high molecular weight polyethylene,¹ structurally related chromium complexes (**A**, Chart 1) have also emerged as effective (pre-)catalysts.² Indeed, chromium as a metal center has a well-documented history for its applications in ethylene oligo-/polymerization with both homogeneous and heterogeneous industrial processes operated.³ With a view to enhancing the catalytic performance of a bis(imino)pyridine-metal catalyst, considerable research effort has been directed towards varying the steric and electronic properties of the ligand framework including through modifications to the *N*-aryl groups. More recently, the introduction of fused cycloalkyl units to the tridentate ligand frame has offered as a further means of influencing the catalyst's effectiveness as well as

having an impact on its thermal stability and the polymer properties.^{4,5} With particular regard to chromium, precatalyst **B** which incorporates two fused cycloheptyl rings (Chart 1), operates efficiently at 80 °C and can form high density polyethylene or polyethylene waxes, depending on the co-catalyst type employed.^{5a} On the other hand, singly fused cyclopentyl-**C** (Chart 1) is more temperature sensitive but forms strictly linear polyethylenes,^{5b} while its cyclohexyl-containing counterpart **D** (Chart 1) shows good thermal stability and generates narrowly dispersed polyethylene of low molecular weight, with high degrees of vinyl unsaturation.^{5c} Based on these brief studies involving chromium, it is apparent that the number of fused units as well as the ring size influence not only catalyst stability but also the polymer chain growth and termination steps.

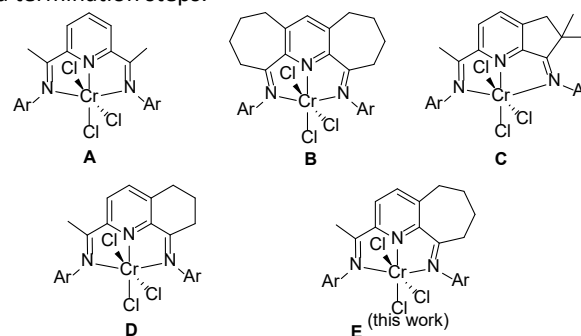


Chart 1 Chromium(III) precatalysts derived from parent bis(imino)pyridine-containing **A**

^a Key Laboratory of Engineering Plastics and Beijing National Laboratory for Molecular Sciences, Institute of Chemistry, Chinese Academy of Sciences, Beijing 100190, China. E-mail: whsun@iccas.ac.cn

^b CAS Research/Education Center for Excellence in Molecular Sciences, University of Chinese Academy of Sciences, Beijing 100049, China

^c College of Chemical Engineering, Zhejiang University of Technology, Hangzhou 310014, China. Email: xinquan@zjut.edu.cn

^d Department of Chemistry, University of Leicester, University Road, Leicester LE1 7RH, UK. E-mail: gas8@leicester.ac.uk

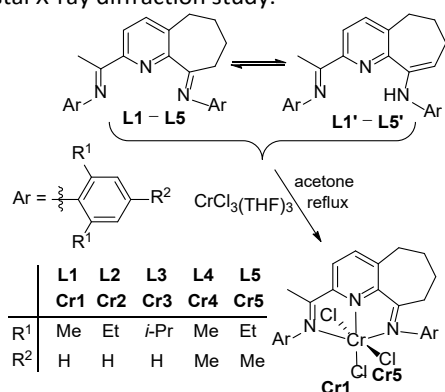
Electronic Supplementary Information (ESI) available: CCDC 1858340 contains the supplementary crystallographic data for complex **Cr2**.

With a view to further investigate the effects of cycloalkyl fusion on the performance of a chromium catalyst, we disclose in this work complexes bearing bis(imino)pyridines fused with a single cycloheptyl ring. In particular, five examples of 2-(1-aryliminoethyl)-9-arylimino-5,6,7,8-tetrahydrocycloheptapyridine-chromium(III) chlorides are reported that differ in both the steric and electronic properties of the *N*-aryl groups (**E**, Chart 1). An in-depth catalytic evaluation of these precatalysts is then conducted to investigate how co-catalyst, temperature, pressure and run time, influence catalyst stability as well as polymer molecular weight, dispersity and degree of vinyl end groups; comparisons with fused **B – D** as well as **A** are also developed. In addition, we explore the ability of the resultant unsaturated polymers to undergo functionalization.

Results and Discussion

Synthesis and Characterization

The chromium(III) complexes, [2-{(Ar)N=CMe}-9-{N(Ar)}C₁₀H₁₀N]CrCl₃ (Ar = 2,6-Me₂C₆H₃ **Cr1**, 2,6-Et₂C₆H₃ **Cr2**, 2,6-*i*-Pr₂C₆H₃ **Cr3**, 2,4,6-Me₃C₆H₂ **Cr4**, 2,6-Et₂-4-MeC₆H₂ **Cr5**), have been prepared in high yields (78 – 90%) by the stoichiometric reactions of the corresponding ligand with CrCl₃(THF)₃ in acetone at reflux (Scheme 1).^{5c} The free ligands themselves exist as a tautomeric mixture consisting of imine 2-{(Ar)N=CMe}-9-{N(Ar)}C₁₀H₁₀N (Ar = 2,6-Me₂C₆H₃ **L1**, 2,6-Et₂C₆H₃ **L2**, 2,6-*i*-Pr₂C₆H₃ **L3**, 2,4,6-Me₃C₆H₂ **L4**, 2,6-Et₂-4-MeC₆H₂ **L5**) and ene-amine 2-{(Ar)N=CMe}-9-{NH(Ar)}C₁₀H₉N (Ar = 2,6-Me₂C₆H₃ **L1'**, 2,6-Et₂C₆H₃ **L2'**, 2,6-*i*-Pr₂C₆H₃ **L3'**, 2,4,6-Me₃C₆H₂ **L4'**, 2,6-Et₂-4-MeC₆H₂ **L5'**); previously reported approaches have been used for their synthesis.^{4e} All five complexes have been characterized by IR spectroscopy and by elemental analysis. In addition, **Cr2** has been the subject of a single crystal X-ray diffraction study.



Scheme 1 Synthetic route to **Cr1 – Cr5**

Single crystals of **Cr2** suitable for the X-ray determination were grown by slow diffusion of heptane into a saturated dichloromethane solution at room temperature. A view of the structure is shown in Figure 1; selected bond lengths and angles are listed in Table 1. The structure of **Cr2** comprises a chromium center bound by three nitrogen donors belonging to **L2** and three chloride ligands to complete a distorted

octahedral geometry. The terdentate ligand adopts a *mer*-configuration with its central pyridine *trans* to Cl3 (N2–Cr1–Cl3 173.04(11)°), while the other two chlorides are *trans* to each other (Cl1–Cr1–Cl2 175.58(5)°); related structural arrangements have been reported previously.^{5,6} Of the three chromium-

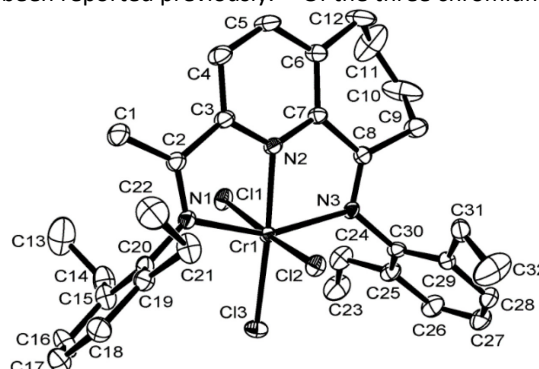


Figure 1 ORTEP representation of **Cr2**. The thermal ellipsoids are shown at the 30% probability level while the hydrogen atoms have been omitted for clarity

Table 1 Selected bond lengths (Å) and angles (°) for **Cr2**

Bond lengths (Å)			
Cr(1)–N(1)	2.134(3)	Cr(1)–Cl(2)	2.2937(12)
Cr(1)–N(2)	2.015(3)	Cr(1)–Cl(3)	2.2886(12)
Cr(1)–N(3)	2.135(3)	N(1)–C(2)	1.301(5)
Cr(1)–Cl(1)	2.3318(12)	N(3)–C(8)	1.280(5)
Bond angles (°)			
N(1)–Cr(1)–N(3)	153.24 (13)	N(2)–Cr(1)–Cl(2)	94.03(11)
N(1)–Cr(1)–N(2)	77.38(14)	N(2)–Cr(1)–Cl(3)	173.04(11)
N(2)–Cr(1)–N(3)	76.62(13)	N(3)–Cr(1)–Cl(1)	90.94(10)
N(1)–Cr(1)–Cl(1)	91.50(10)	N(3)–Cr(1)–Cl(2)	88.88(10)
N(1)–Cr(1)–Cl(2)	86.69(10)	N(3)–Cr(1)–Cl(3)	103.79(10)
N(1)–Cr(1)–Cl(3)	102.79(10)	C(2)–N(1)–Cr(1)	114.3(3)
N(2)–Cr(1)–Cl(1)	81.64(11)	C(8)–N(3)–Cr(1)	115.1(3)

nitrogen distances, the exterior Cr–N_{imine} distances are the longest and, despite their distinct imine environments, similar in length (Cr1–N1 2.134(3) Å, Cr1–N3, 2.135(3) Å). In comparison with related iron(II) and cobalt(II) structures, the Cr–N_{pyridine} bond length (Cr1–N2 2.015(3) Å) in **Cr2** is shorter [Fe–N_{pyridine} (2.107 Å),^{4e} Co–N_{pyridine} (2.051 Å)^{4f}], reflecting the more effective binding with the higher oxidation state Cr(III) center.^{5c} The two N-aryl rings are inclined at angles of 74.46° and 78.19° with respect to their neighbouring imine vectors in a manner similar to that seen in similar structures.⁵ The C9–C10–C11–C12 section of the fused cycloheptyl unit adopts a puckered arrangement as a result of their sp³-hybridized carbon atoms. There are no intramolecular contacts of note.

By comparison to **L1/L1' – L5/L5'**,^{4e} the IR spectra of **Cr1 – Cr5** showed clear shifts in their ν_{C=N} stretching vibrations to lower wavenumber, in agreement with effective coordination between the imine-nitrogen and the chromium center. Furthermore, there was no evidence for any N–H stretching bands in the IR spectra, confirming the tridentate ligand adopts solely the bis(imine) form on coordination.^{5c} Their elemental analyses were consistent with complexes of composition LCrCl₃.

Ethylene Polymerization

Based on previous studies of structurally similar *N,N,N*-bound chromium(III) complexes, methylaluminumoxane (MAO) and modified methylaluminumoxane (MMAO) have proved the most

effective co-catalysts to promote ethylene polymerization.^{5c} Hence this study is concerned with an evaluation of these two aluminumoxanes using **Cr2** as the test precatalyst to allow an

Table 2 Ethylene polymerization using **Cr1** – **Cr5**/MMAO^a

Entry	Precat.	T (°C)	Al:Cr	t (min)	Mass (g)	Activity ^b	M_w^c	M_w/M_n^c	T_m (°C) ^d	X_c (%) ^d
1	Cr2	20	2000	30	0.94	0.63	0.66	1.14	83.6	50.1
2	Cr2	30	2000	30	1.99	1.33	0.80	1.26	90.3	55.2
3	Cr2	40	2000	30	3.31	2.21	0.98	1.33	90.6	51.2
4	Cr2	50	2000	30	7.09	4.73	2.88	2.01	102.3	73.5
5	Cr2	60	2000	30	12.24	8.16	2.35	1.81	124.5	76.7
6	Cr2	70	2000	30	14.77	9.85	2.25	1.83	122.8	82.0
7	Cr2	80	2000	30	12.14	8.09	1.59	1.49	122.5	75.8
8	Cr2	90	2000	30	6.16	4.11	1.49	1.47	116.5	77.8
9	Cr2	100	2000	30	0.57	0.38	1.41	1.43	122.5	79.0
10	Cr2	70	1500	30	8.37	5.58	2.87	1.86	124.3	85.5
11	Cr2	70	1750	30	13.13	8.75	2.22	1.68	122.9	81.7
12	Cr2	70	2250	30	13.36	8.91	2.76	1.76	123.2	78.2
13	Cr2	70	2500	30	9.60	6.40	2.58	1.85	124.0	82.4
14	Cr2	70	2000	5	2.53	10.12	1.06	1.34	109.1	72.7
15	Cr2	70	2000	15	8.80	11.73	1.99	1.63	120.4	73.5
16	Cr2	70	2000	45	18.46	8.20	2.99	1.96	124.9	79.3
17	Cr2	70	2000	60	20.03	6.68	3.56	2.05	125.8	83.2
18 ^e	Cr2	70	2000	30	9.05	6.03	1.98	1.75	120.3	68.3
19 ^f	Cr2	70	2000	30	0.27	0.18	0.57	1.25	71.7	45.0
20	Cr1	70	2000	30	19.26	12.84	1.59	1.75	117.6	79.5
21	Cr3	70	2000	30	0.28	0.19	2.72	2.05	123.6	76.0
22	Cr4	70	2000	30	9.93	6.62	0.90	1.42	107.6	66.0
23	Cr5	70	2000	30	6.15	4.10	1.11	1.56	111.2	75.6

^a General conditions: 3 μmol of precatalyst, 10 atm C_2H_4 , 100 mL of toluene; ^b $\times 10^6$ g (PE)·mol⁻¹ (Cr)·h⁻¹; ^c M_w in kg·mol⁻¹, determined by GPC;

^d Determined by DSC; crystallinity based on $\Delta H_m = 293$ J·g⁻¹ for a 100% crystalline PE; ^e 5 atm C_2H_4 ; ^f 1 atm C_2H_4 .

optimization of the conditions with each co-catalyst. Typically, the polymerizations were performed in toluene at 10 atm C_2H_4 . All the polymers were characterized by gel permeation chromatography (GPC) and differential scanning calorimetry (DSC). In addition, high temperature NMR spectroscopy was employed to examine the microstructural properties of selected polymer samples. In each case gas chromatography (GC) was performed to check for any oligomeric fractions generated during the runs.

(a) Catalytic evaluation of **Cr1** – **Cr5**/MMAO

To ascertain the optimal polymerization conditions using the **Cr2**/MMAO combination, the run temperature, the Al:Cr molar ratio and run time were all systematically varied; the results of the runs are collected in Table 2. Firstly, with the Al:Cr molar ratio fixed at 2000, the reaction temperature was raised from 20 to 100 °C leading to a peak in activity of 9.85×10^6 g (PE) mol⁻¹ (Cr) h⁻¹ being recorded at 70 °C (entries 1 – 9, Table 2); further increasing the temperature to 80 °C saw a modest drop in performance before a more dramatic loss in activity was observed as the temperature was raised further (entries 6 – 9, Table 2). The lowest molecular weights (M_w : 0.66 – 0.98 kg·mol⁻¹) and narrowest distributions ($M_w/M_n = 1.14$ – 1.33) were generated at the lower reaction temperatures (20 – 40 °C, entries 1 – 3, Table 2), which could be due to the slow rates

of chain propagation and chain transfer under these conditions.^{5c} However, further increasing the temperature saw a peak in M_w of 2.88 kg·mol⁻¹ at 50 °C, above which the molecular weight gradually declined reaching its lowest point of 1.41 kg·mol⁻¹ at 100 °C. This reduction in molecular weight is probably due to the onset of decomposition of the active species at elevated temperatures. The GPC curves of the polymers obtained under various reaction temperatures are illustrated in Figure 2a, while plots of activity/molecular weight versus reaction temperature are depicted in Figure 2b. Despite the wide range in reaction temperatures being investigated (20 – 100 °C), all the polymers exhibited narrow unimodal distributions which is consistent with single site species.

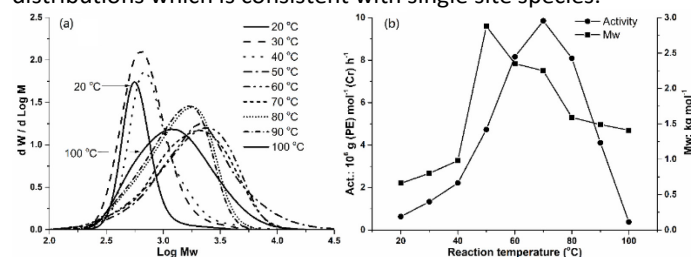


Figure 2 (a) GPC curves of the polyethylenes formed using **Cr2**/MMAO at various temperatures; (b) plot of activity and M_w vs. reaction temperature for the same catalyst (entries 1 – 9, Table 2)

Secondly, with the temperature set at 70 °C, the Al:Cr molar ratio was varied from 1500 to 2500 using **Cr2**/MMAO (entries 6, 10 – 13, Table 2). The catalytic activity reached a maximum of 9.85×10^6 g (PE) mol⁻¹ (Cr) h⁻¹ at a molar ratio of 2000 and then steadily decreased as the ratio was raised to 2500. This latter observation could plausibly be attributed to increased chain transfer to aluminum occurring with larger amounts of co-catalyst.⁵ However, the molecular weights of the resultant polyethylenes did not show any significant variation with the values falling in the range 2.22 – 2.87 kg·mol⁻¹.

Thirdly, the lifetime of active catalyst was examined by performing the polymerizations over 5, 15, 30, 45 and 60 minutes with the temperature maintained at 70 °C and the Al:Cr molar ratio at 2000. The topmost activity of 11.73×10^6 g (PE)·mol⁻¹ (Cr)·h⁻¹ was observed after 15 minutes and then gradually decreased with more extended run times (entries 6 and 14 – 17, Table 2), highlighting the slow induction period needed to form the active species followed by the onset of catalyst deactivation over time. Furthermore, the molecular weights of the polyethylenes displayed a gradual increase as the reaction time was prolonged indicating that despite apparent deactivation there were sufficient active species to maintain chain propagation (Figure 3). On reducing the ethylene pressure from 10 atm to firstly 5 atm and then to 1 atm, with the other reaction parameters unchanged, inferior catalytic activity and lower molecular weight polyethylenes were observed (entries 18 and 19, Table 2).⁵

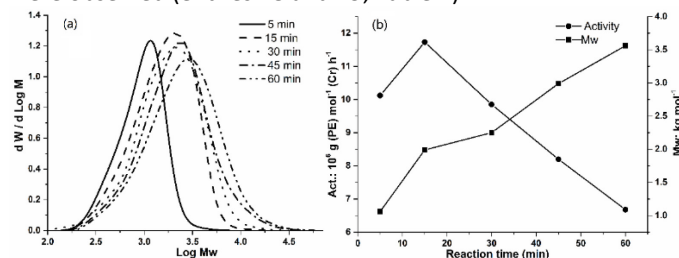


Figure 3 (a) GPC curves for the polyethylenes obtained using **Cr2**/MMAO at various run times; (b) plot of activity and M_w vs. reaction time for the same catalyst (entries 6 and 14 – 17, Table 2)

Finally, using the optimal polymerization conditions established for **Cr2** (viz., Al:Cr ratio of 2000, reaction temperature of 70 °C and 30 minute run time), the remaining four precatalysts were evaluated and their results discussed alongside **Cr2** (entries 6 and 20 – 23, Table 2). In general, all complexes showed high catalytic activities with the exception of

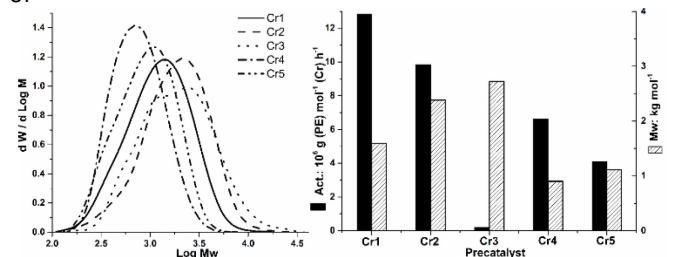


Figure 4 (a) GPC curves of the polymers generated using **Cr1** – **Cr5**/MMAO; (b) comparative activity of **Cr1** – **Cr5** and M_w of the corresponding polymers (entries 6 and 20 – 23, Table 2)

Cr3 and fall in the order: **Cr1** [2,6-di(Me)] > **Cr2** [2,6-di(Et)] > **Cr4** [2,4,6-tri(Me)] > **Cr5** [2,6-di(Et)-4-Me] >> **Cr3** [2,6-di(*i*-Pr)]. These variations in activity can be explained in terms of both steric and electronic properties of the precatalyst. For example, the most sterically bulky 2,6-diisopropyl-substituted **Cr3** gave the lowest activity (0.19×10^6 g (PE) mol⁻¹ (Cr) h⁻¹), while the least bulky **Cr1** the highest (12.84×10^6 g (PE) mol⁻¹ (Cr) h⁻¹). It is evident that the more bulky groups impede ethylene coordination leading to lower polymerization rates.^{5c} The presence of an electron donating *para*-methyl group in **Cr4** and **Cr5** appears to have a detrimental effect on activity when compared to their closest comparators **Cr1** and **Cr2**; similar electronic effects have been noted elsewhere.^{5c} In terms of the molecular weight of the polymer, steric and electronic effects are again influential with the most bulky system **Cr3** delivering the highest molecular weight polymer (Figure 4). On the other hand, the *para*-methyl precatalysts **Cr4** and **Cr5** form polymers exhibiting the lowest molecular weight and the narrowest distributions. Indeed, all the polymers show narrow distributions though **Cr3** shows some evidence for a bimodal distribution with a slight shoulder in its GPC trace (Figure 4a).

Based on the melt temperatures (T_m range = 110 – 130 °C) and high crystallinities of the polymers, these materials can be described in general as adopting highly linear structures. To confirm this conclusion, one representative polymer sample prepared using **Cr2**/MMAO at 70 °C (entry 6, Table 2) was investigated by high temperature NMR spectroscopy (in 1,1,1,2-tetrachloroethane-*d*₂ at 100 °C). Examination of the ¹H NMR and ¹³C NMR spectra reveals prominent singlets at respectively δ 1.35 (Figure 5) and δ 30.00 (d, Figure 6), corresponding to the -(CH₂)_n- repeat unit, chemical shifts that are indeed typical of a strictly linear polyethylene. Furthermore, the ¹H NMR spectrum shows less intense downfield peaks at δ 5.90 and 5.00, with relative integrals of 1:2, that are characteristic of a terminal vinyl group (-CH=CH₂); the corresponding vinylic carbons are seen at δ 139.34 (f, Figure 6) and 114.39 (g, Figure 6) in the ¹³C NMR spectrum. The terminal methyl group in the ¹H NMR spectrum is also visible at δ 0.90 while the corresponding propyl resonances (a, b and c, Figure 6) can be seen at δ 14.26, 22.93 and 32.24 in the ¹³C NMR spectrum. Comparison of the integrals for the upfield methyl (*ca.* 7.7) with the vinylic protons (1:2) in the ¹H NMR spectrum would suggest the presence of some fully saturated polymer. However, quantification of the relative amounts of these classes of polymers could not be determined with any accuracy due to the overlapping of the signals for the methyl and -(CH₂)- protons. Nonetheless, such vinyl unsaturation is consistent with a termination pathway involving β -hydrogen elimination or transfer to monomer, while the likely presence of saturated polymer can be accounted for by a termination pathway involving chain transfer to aluminum in the co-catalyst.^{4e,4i,7}

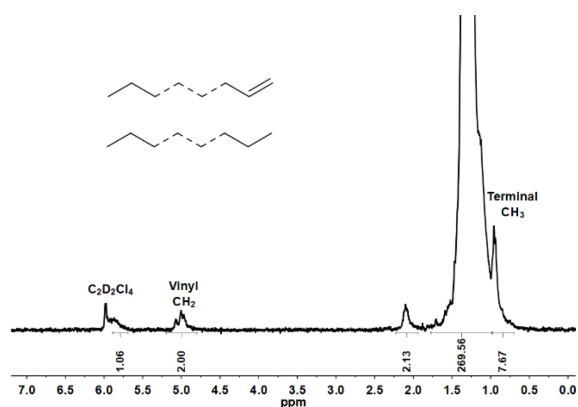


Figure 5 ^1H NMR spectrum of the polyethylene obtained using **Cr2**/MAAO at 70 °C (entry 6, Table 2); recorded in 1,1,2,2-tetrachloroethane- d_2 at 100 °C

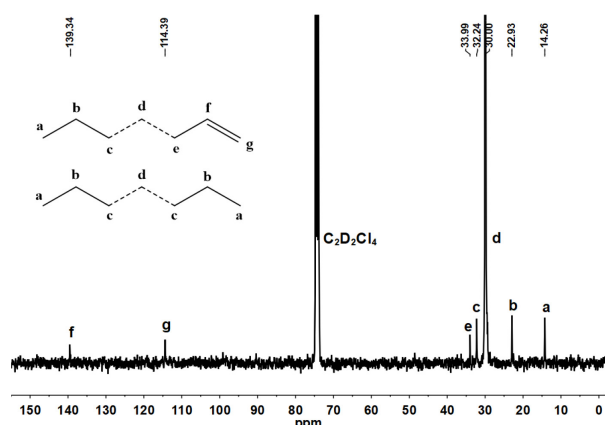


Figure 6 ^{13}C NMR spectrum of the polyethylene obtained using **Cr2**/MAAO at 70 °C (entry 6, Table 2); recorded in 1,1,2,2-tetrachloroethane- d_2 at 100 °C

(b) Catalytic evaluation of **Cr1** – **Cr5**/MAO

As with the MMAO study, **Cr2** was again used to optimize the polymerization conditions this time employing MAO as the co-catalyst; the results are compiled in Table 3. In a similar manner, the polymerizations were initially conducted between 20 and 100 °C with the Al:Cr molar ratio fixed at 2000 and the run time at 30 minutes. In contrast to **Cr2**/MMAO, the highest catalytic activity of **Cr2**/MAO was reached at 80 °C (9.19×10^6 g (PE) mol^{-1} (Cr) h^{-1}) and even up to 100 °C this system displayed greater productivity reflecting its superior thermal stability. On the other hand, at lower reaction temperature (20 – 30 °C) the activity of **Cr2**/MAO was markedly less.

With the temperature retained at 80 °C, the molar Al:Cr ratio was varied between 2000 and 3000 resulting in a peak activity of 10.85×10^6 g (PE) mol^{-1} (Cr) h^{-1} being achieved with a ratio of 2500 (*c.f.* 2000 for **Cr2**/MMAO). Notably, over a run time of 5 minutes **Cr2**/MAO exhibited the highest activity (15.72×10^6 g (PE) mol^{-1} (Cr) h^{-1}) of the entire study (entry 14, Table 3), highlighting the relatively short induction period needed for this catalyst system (*c.f.* with 15 minutes for **Cr2**/MMAO).^{5,8}

With regard to polyethylenes generated using **Cr2**/MAO, all materials displayed unimodal distributions in spite of variations in either temperature or in the Al:Cr molar ratio (M_w/M_n : 1.22 – 2.00, see Figure S1). Likewise, over the 5 – 60

minutes run time, little deviation from single-site behavior was observed. In terms of molecular weight, the lowest M_w value and narrowest distribution was observed at 30 °C while the highest molecular weight of the polyethylenes was obtained at 60 °C ($3.48 \text{ kg}\cdot\text{mol}^{-1}$, entry 5, Table 3).

With the optimum catalytic conditions established for **Cr2**/MAO (*viz.*, Al:Cr molar ratio of 2500, temperature of 80 °C and run time of 30 minutes), the remaining four chromium complexes **Cr1**, **Cr3**, **Cr4** and **Cr5** were screened (entries 20 – 23, Table 3). Overall, the results were similar to those observed with **Cr1** – **Cr5**/MMAO with the catalytic activities decreasing in the order: **Cr1** [2,6-di(Me)] > **Cr2** [2,6-di(Et)] > **Cr4** [2,4,6-tri(Me)] > **Cr5** [2,6-di(Et)-4-Me] > **Cr3** [2,6-di(*i*-Pr)] (Figure S2). Once again **Cr3** proved the least active but yielded polymers exhibiting the highest molecular weight, a finding that is in accordance with the increased steric bulk at the active center leading to a decrease in the rate of chain transfer relative to propagation. Interestingly, the apparent bimodal distribution first noted using **Cr3**/MMAO, is now more prominent with **Cr3**/MAO (Figure S2a). It is uncertain as to content of the two fractions of this polymer, but it may be due to the saturated and unsaturated polymers in this case possessing visibly different molecular weights.⁴ⁱ

To confirm the linearity of the polymers (T_m range = 115.4 – 125.8 °C), a sample prepared using **Cr2** and 2500 molar equivalents of MAO at 80 °C was subjected to high temperature NMR spectroscopy (entry 11, Table 3). As observed earlier, the ^1H and ^{13}C NMR spectra gave signals characteristic of linear polymers as well as less intense signals corresponding to a vinylic end group, again highlighting the importance of β -hydrogen elimination/transfer as one possible termination pathway (Figures S3 and S4).

Vinyl content of the polymers and their functionalization

With the aim to investigate the effect of polymerization conditions on the relative percentage of vinyl-terminated to fully saturated polymers, several samples generated using different reaction conditions were studied using high temperature ^1H NMR spectroscopy. Firstly, the effect of temperature was explored with the Al:Cr ratio maintained at 2000. Inspection of Figure 7 reveals a steady decrease in the vinyl content as the temperature was raised from 50 to 100 °C (77.4% at 50 °C, 75.6% at 80 °C and 61.1% at 100 °C), which suggests a preference for chain transfer to aluminum as the temperature of the polymerization was increased. Secondly, with the temperature kept at 80 °C and the Al:Cr ratio increased to 2500 (entry 11, Table 3), the vinyl content slightly reduced to 74.3%, as would be expected with the presence of more alkyl-aluminum co-catalyst (Figure S3). Thirdly, the effect of time and pressure were explored with the Al:Cr molar ratio retained at 2500 and the temperature at 80 °C. With respect to time, the vinyl content reaches a maximum after 45 minutes and then decreases after one hour (64.0% at 5 min, 66.6% at 15 min, 74.3% at 30 min, 78.4% at 45 min and 69.0% at 60 min, Figure 8). With the pressure reduced to 5 atm C_2H_4 and then 1 atm, 50.7% and 41.0% vinyl content was achieved, respectively, after 30 minutes (*c.f.* 74.3% at 10 atm),

suggesting that chain transfer to aluminum is favoured at lower pressure (Figure 9).

Table 3 Ethylene polymerization using Cr1 – Cr5/MAO^a

Entry	Precat.	T (°C)	Al:Cr	t (min)	Mass (g)	Activity ^b	M_w^c	M_w/M_n^c	T_m (°C) ^d	X_c (%) ^d
1	Cr2	20	2000	30	trace	–	–	–	–	–
2	Cr2	30	2000	30	0.38	0.25	0.81	1.22	92.3	72.8
3	Cr2	40	2000	30	2.40	1.60	2.05	1.88	123.1	81.4
4	Cr2	50	2000	30	7.05	4.70	2.28	1.89	124.8	81.4
5	Cr2	60	2000	30	8.98	5.99	3.48	2.00	125.8	81.6
6	Cr2	70	2000	30	11.35	7.67	2.91	1.86	124.6	78.3
7	Cr2	80	2000	30	13.79	9.19	2.67	1.85	124.3	78.9
8	Cr2	90	2000	30	9.41	6.27	2.56	1.80	123.7	73.6
9	Cr2	100	2000	30	2.91	1.94	1.53	1.52	121.5	76.8
10	Cr2	80	2250	30	15.01	10.01	3.17	1.98	125.0	79.1
11	Cr2	80	2500	30	16.28	10.85	2.83	1.84	123.6	77.9
12	Cr2	80	2750	30	15.70	10.47	2.96	1.95	123.7	77.8
13	Cr2	80	3000	30	14.81	9.87	3.01	1.85	123.9	76.3
14	Cr2	80	2500	5	3.96	15.72	2.38	1.77	123.4	78.9
15	Cr2	80	2500	15	8.67	11.56	2.65	1.87	123.0	74.8
16	Cr2	80	2500	45	18.16	8.07	3.18	2.01	124.9	80.5
17	Cr2	80	2500	60	20.04	6.68	3.00	1.93	124.5	79.3
18 ^e	Cr2	80	2500	30	5.29	3.53	1.67	1.61	121.5	81.2
19 ^f	Cr2	80	2500	30	0.79	0.53	1.23	1.54	103.6	76.6
20	Cr1	80	2500	30	21.66	14.44	1.93	1.80	120.4	78.6
21	Cr3	80	2500	30	0.36	0.24	3.21	2.62	125.5	70.9
22	Cr4	80	2500	30	17.46	11.64	1.51	1.75	117.2	75.9
23	Cr5	80	2500	30	7.84	5.23	1.34	1.54	115.4	76.3

^a General conditions: 3 μ mol of precatalyst; 10 atm C₂H₄; 100 mL of toluene; ^b $\times 10^6$ g (PE)-mol⁻¹ (Cr)-h⁻¹; ^c M_w in kg·mol⁻¹, determined by GPC; ^d Determined by DSC; crystallinity based on $\Delta H_m = 293$ J·g⁻¹ for a 100% crystalline PE; ^e 5 atm C₂H₄; ^f 1 atm C₂H₄.

To explore the amenability of a low molecular weight polymer sample containing a high level of end-group unsaturation to undergo functionalization, the material generated using Cr2/MAO at 80 °C (run 11, Table 3: vinyl content = 74.3%) was employed as a substrate in epoxidation. Indeed, many efforts have been devoted to polyethylene functionalization, aiming to introduce polar/reactive groups into the polymeric chains.^{9,10} *meta*-Chloroperbenzoic acid (*m*-CPBA), was chosen to facilitate the transformation to the epoxy-terminated polyethylene (e-PE) and the conversion determined by NMR spectroscopy.^{9d,11} Examination of the ¹H NMR spectrum of e-PE indicated that the vinyl signals at δ 5.0 and 5.9 had completely disappeared, and three new peaks at δ 2.46, 2.74 and 2.90 corresponding to the proton environments of an epoxide group had appeared (Figure 10). The ¹³C NMR spectrum further confirmed the formation of an epoxide with the disappearance of the vinyl carbon resonances at δ 114.4 and 139.3 and the emergence of two new peaks at δ 47.10 and 52.52 corresponding to the carbon atoms in a three-membered epoxide ring (h and g in Figure 11). It is noteworthy that the ring-opening of such epoxide-terminated polyethylene have been the subject of a number of investigations.^{9d,12}

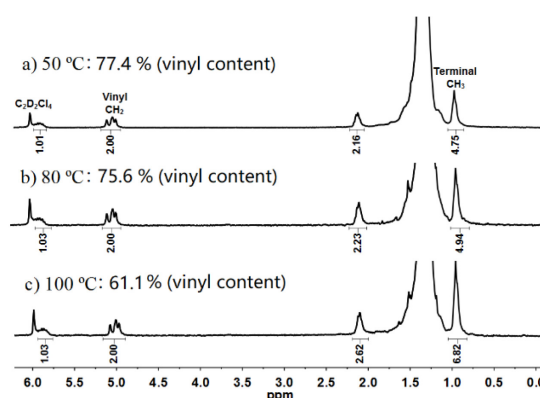


Figure 7 ¹H NMR spectra of the polyethylene generated at 50, 80 and 100 °C using Cr2/MAO (entries 4, 7 and 9, Table 3); recorded in 1,1,2,2-tetrachloroethane-*d*₂ at 100 °C

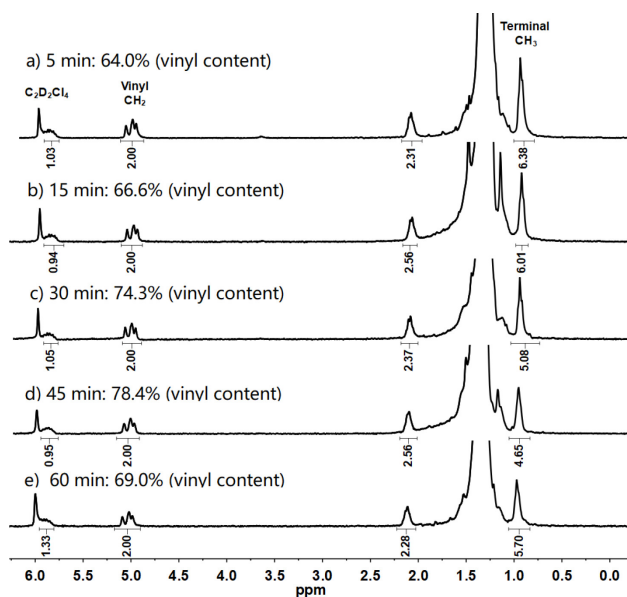


Figure 8 ^1H NMR spectra of the polyethylene generated after a) 5, b) 15, c) 30, d) 45, e) 60 minutes using Cr_2/MAO (entries 14, 15, 11, 16 and 17, Table 3); recorded in 1,1,2,2-tetrachloroethane- d_2 at 100 °C

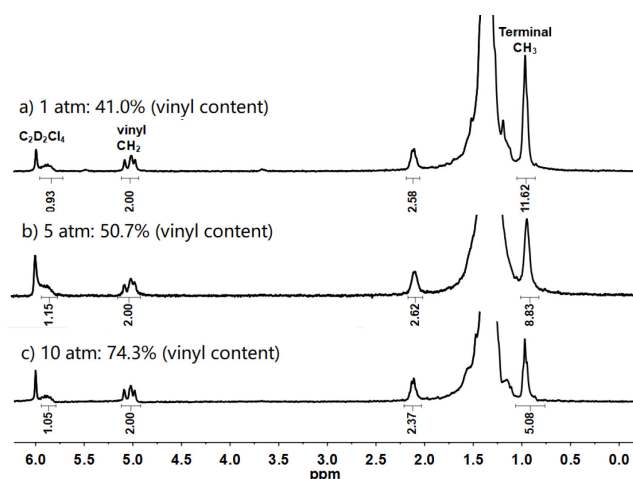


Figure 9 ^1H NMR spectra of the polyethylene generated at a) 1, b) 5 and c) 10 atm C_2H_4 using Cr_2/MAO (entries 19, 18 and 11, Table 3); recorded in 1,1,2,2-tetrachloroethane- d_2 at 100 °C

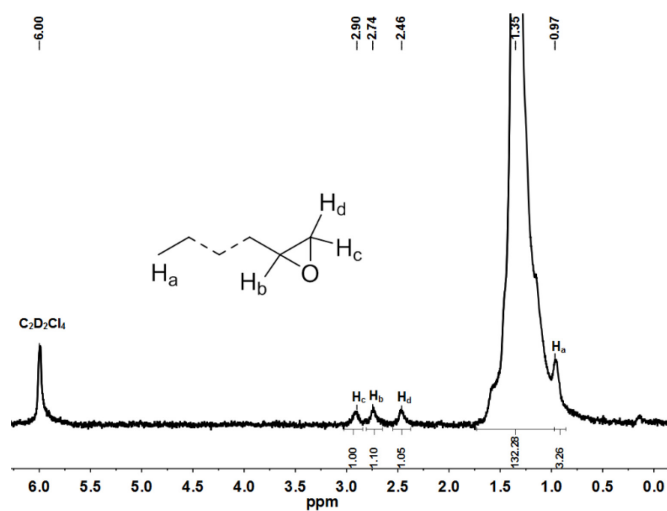


Figure 10 ^1H NMR spectrum of the e-PE; recorded in 1,1,2,2-tetrachloroethane- d_2 at 100 °C

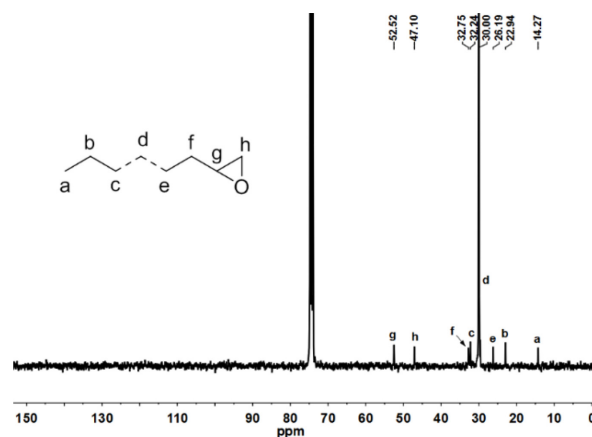


Figure 11 ^{13}C NMR spectrum of the e-PE; recorded in 1,1,2,2-tetrachloroethane- d_2 at 100 °C

Comparative performance of Cr_2 with other fused ring and related catalysts

To allow a more general comparison of the performance of the catalysts developed in this study, the activity and molecular weight data of the polymers obtained using chromium-containing **A**/MMAO, **B**/MMAO and **D**/MMAO (Ar = 2,6-Et $_2$ C $_6$ H $_3$, Chart 1) at 10 atm C_2H_4 and 80 °C, are presented alongside Cr_2 /MMAO (entry 7, Table 2) in Figure 12; additional data are collected in Table S1. To maintain comparable conditions, the polymerization data for **A** and **C** had to be re-collected under the stated conditions as lower pressure or lower reaction temperatures had previously been reported.^{3,5b} Unfortunately, **C** under these conditions showed only trace activity, on account of its poor thermal stability and thus is not included in Figure 12 (entry 3, Table S1). Nevertheless, this result does highlight the importance of the *N,N*-chelating ligand on catalytic performance; the ineffective chelation properties of this strained ligand in **C** are likely responsible for catalyst deactivation (the $N_{\text{imine}}\text{-Cr}$ distances are 2.299 and 2.150 Å).^{5b,5c} Inspection of the figure reveals that parent **A** generates the lowest activity and the lowest molecular weight polyethylene. On the other hand, fused **B**, **D** and Cr_2 are not only more active ($\text{D} > \text{Cr}_2 > \text{B}$) but form higher molecular weight polyethylene ($\text{B} > \text{Cr}_2 > \text{D}$). It would appear that these less strained fused 2,6-bis(imino)pyridines in **B**, **D** and Cr_2 are more effective chelating ligands and provide better protection and stability to the active species at higher polymerization temperatures. Collectively, these data further emphasize the pronounced effect of the fused ring size on the activity of catalyst and the molecular weight of the polymer.

Furthermore, the catalytic performance of Cr_2 /MMAO has been compared with its closest iron and cobalt comparators, **Fe2** and **Co2**, respectively under similar reaction conditions (Table 4). Two key points emerge from examination of the data. Firstly, Cr_2 displays its optimal activity at the highest temperature underlining the good thermal stability of this system. Nevertheless, the Cr_2 system is not as active as the iron catalyst but is more active than its cobalt derivative. Secondly, the molecular weight of the polyethylene obtained using Cr_2 is the

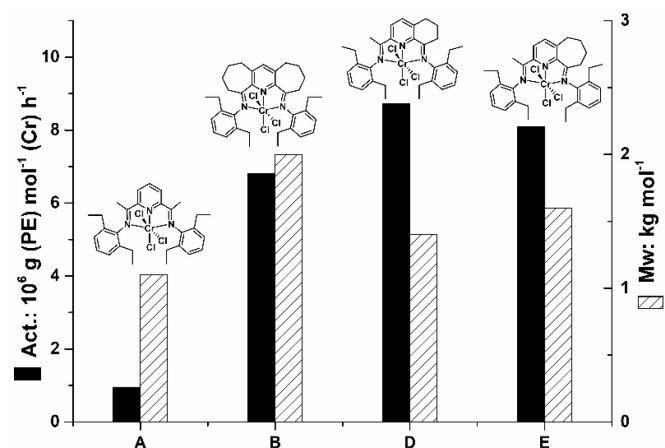


Figure 12 Comparative catalytic performance of **Cr2** (**E**) with **A**,³ **B**,^{5a} and **D**^{5c} (Chart 1); all runs conducted using MMAO as co-catalyst, $P_{\text{C}_2\text{H}_4} = 10 \text{ atm}$ and at $80 \text{ }^\circ\text{C}$

Table 4 Performance data for structurally related iron, cobalt and chromium precatalysts; all polymerizations conducted using MMAO and $10 \text{ atm C}_2\text{H}_4$ ^a

Precatalyst			
Optimal activity ($\text{g (PE) mol}^{-1} (\text{M}) \text{ h}^{-1}$)	14.0×10^6	1.7×10^6	9.85×10^6
Optimal temp. ($^\circ\text{C}$)	50	50	70
M_w ($\text{kg}\cdot\text{mol}^{-1}$) ^b	11.5	7.2	2.4
M_w/M_n ^b	5.9	2.2	1.8
T_m ($^\circ\text{C}$) ^c	128.2	128.4	122.8

^a General conditions: $10 \text{ atm C}_2\text{H}_4$, 100 mL of toluene; ^b Determined by GPC; ^c Determined by DSC.

lowest of this series and displays the narrowest molecular weight distribution; an observation that has also been noted with analogous Fe, Co, and Cr complexes bearing 2-[1-(arylimino)ethyl]-8-arylimino-5,6,7-trihydroquinoline ligands.^{5c}

Conclusions

The cycloheptyl-fused bis(arylimino)pyridine-chromium(III) chloride complexes, **Cr1** – **Cr5**, have been successively synthesized and fully characterized. The molecular structure of *N*-diethylphenyl-containing **Cr2** has also been determined by single-crystal X-ray diffraction. On activation with MAO or MMAO, all the chromium complexes exhibited high activities for ethylene polymerization at elevated operating temperatures with the least sterically encumbered **Cr1** the most productive at $14.44 \times 10^6 \text{ g (PE)}\cdot\text{mol}^{-1} (\text{Cr})\cdot\text{h}^{-1}$. Moreover, the polymers are linear, of low molecular weight and display narrow dispersities. In addition, high levels of vinyl chain ends are a feature along with lower levels of fully saturated end-groups, their relative weightings being influenced by temperature, pressure and amount of aluminoxane co-catalyst. It has also been demonstrated that these vinyl-terminated polymers can be readily converted to their epoxide-terminated counterparts. In comparison to iron and

cobalt catalysts bearing the same fused *N,N,N* ligand, the current family of chromium catalysts offer greater thermal stability while still maintaining high catalytic activity and produce lower molecular weight material. We are currently exploring further applications of these vinyl-terminated polyethylene waxes.

Experimental Section

General procedures

All operations including air and/or moisture sensitive compounds were performed under an atmosphere of nitrogen using standard Schlenk techniques. Prior to use, toluene was refluxed over sodium-benzophenone and distilled under nitrogen. Methylaluminumoxane (MAO, 1.46 M solution in toluene) and modified methylaluminumoxane (MMAO, 2.0 M solution in *n*-heptane) were purchased from Akzo Nobel Corp. High-purity ethylene was purchased from Beijing Yanshan Petrochemical Co. and used as received. Other reagents were purchased from Aldrich, Acros or local suppliers. NMR spectra were recorded on a Bruker DMX 400 MHz instrument at ambient temperature using TMS as an internal standard. IR spectra were recorded on a Perkin-Elmer System 2000 FT-IR spectrometer, while elemental analyses were measured on a Flash EA 1112 microanalyzer. Molecular weights (M_w) and molecular weight distributions (M_w/M_n) of the polyethylenes were measured using an Agilent PL-GPC220 GPC/SEC high temperature system equipped with three $300 \times 7.5 \text{ mm}$ PL gel $10 \mu\text{m}$ MIXED-B LS columns connected in series. The measurements were undertaken at $150 \text{ }^\circ\text{C}$ with a flow rate of $1.0 \text{ mL}\cdot\text{min}^{-1}$ with 1,2,4-trichlorobenzene (TCB) as the eluent. Data collection and handling were carried out using Cirrus GPC Software and Multi Detector Software; data were collected at 1 point per second. The GPC calibration was undertaken using a Polystyrene Calibration Kit S-M-10 supplied by PL Company. The true average molecular weights were determined by inputting the Mark-Houwink constants for polyethylene namely K of 0.727 and α of 40.6 (both provided by PL Company). Samples were dissolved at a concentration of $0.5 - 2.5 \text{ mg}\cdot\text{mL}^{-1}$, depending on the molecular weights. The melt temperatures of the polyethylenes were measured from the second scanning run on a PerkinElmer TA-Q2000 differential scanning calorimeter (DSC) under a nitrogen atmosphere. In the procedure, a sample of about 5.0 mg was heated to $160 \text{ }^\circ\text{C}$ at a rate of $20 \text{ }^\circ\text{C}/\text{min}$ and kept for 2 min at $160 \text{ }^\circ\text{C}$ to remove the thermal history and then cooled at a rate of $20 \text{ }^\circ\text{C}/\text{min}$ to $-40 \text{ }^\circ\text{C}$. ^{13}C NMR spectra of the polyethylenes were recorded on a Bruker DMX 300 MHz instrument at $100 \text{ }^\circ\text{C}$ in deuterated 1,1,2,2-tetrachloroethane with TMS as an internal standard. A VARIAN CP-3800 gas chromatograph equipped with a flame ionization detector and a 30 m column (0.2 mm inner diameter, $0.25 \mu\text{m}$ film thickness) was employed to detect any oligomers from the reaction mixture. Compounds **L1/L1'** – **L5/L5'**,^{4e} $\text{CrCl}_3(\text{THF})_3$ ¹³ and 2,6-bis(diethylphenylimino)pyridine-chromium(III) chloride (**A**, Chart 1)^{3,5b} were synthesized using previously reported procedures.

Synthesis of [2-{(Ar)N=CMe}-9-{N(Ar)}C₁₀H₁₀N]CrCl₃ (Cr1 – Cr5)

(a) *Ar* = 2,6-Me₂C₆H₃ **Cr1**. CrCl₃(THF)₃ (0.188 g, 0.50 mmol) was added to a tautomeric mixture of **L1** and **L1'** (0.246 g, 0.60 mmol) in acetone (10 mL). The solution was stirred and heated to reflux for 5 h and then allowed to cool to room temperature. Excess diethyl ether was poured onto the reaction mixture and the resulting precipitate collected by filtration, washed with diethyl ether (3 × 5 mL) and dried under reduced to give **Cr1** as a brown powder (0.256 g, 90%). FT-IR (cm⁻¹): 2963 (m), 2924 (m), 2869 (m), 1695 (w), 1620 (m, ν_{C=N}), 1578 (s), 1528 (s), 1472 (vs), 1379 (m), 1271 (m), 1250 (w), 1185 (w), 1095 (w), 1033 (w), 893 (w), 833 (w), 771 (vs), 661 (m). Anal. Calcd for C₂₈H₃₁N₃Cl₃Cr (567.92): C, 59.22; H, 5.50; N, 7.40%. Found: C, 58.98; H, 5.56; N, 7.23%.

(b) *Ar* = 2,6-Et₂C₆H₃ **Cr2**. Based on the procedure and molar ratios described for **Cr1** but using **L2/L2'** (0.280 g, 0.60 mmol) and CrCl₃(THF)₃ (0.188 g, 0.50 mmol), **Cr2** was isolated as a green powder (0.275 g, 88%). FT-IR (cm⁻¹): 2958 (m), 2873 (m), 1706 (w), 1614 (m, ν_{C=N}), 1558 (s), 1459 (vs), 1369 (m), 1326 (m), 1264 (m), 1228 (m), 1188 (m), 1127 (m), 999 (w), 852 (w), 807 (s), 777 (vs). Anal. Calcd for C₃₂H₃₉N₃Cl₃Cr (624.03): C, 61.59; H, 6.30; N, 6.73%. Found: C, 61.38; H, 6.38; N, 6.55%.

(c) *Ar* = 2,6-*i*-Pr₂C₆H₃ **Cr3**. Based on the procedure and molar ratios described for **Cr1** but using **L3/L3'** (0.313 g, 0.60 mmol) and CrCl₃(THF)₃ (0.188 g, 0.50 mmol), **Cr3** was isolated as a brown powder (0.292 g, 86%). FT-IR (cm⁻¹): 2961 (m), 2870 (s), 1699 (w), 1623 (m, ν_{C=N}), 1559 (s), 1513 (s), 1462 (vs), 1365 (m), 1326 (m), 1260 (m), 1186 (m), 1125 (w), 1052 (w), 850 (m), 803 (s), 775 (m). Anal. Calcd for C₃₆H₄₇N₃Cl₃Cr (680.14): C, 63.57; H, 6.97; N, 6.18%. Found: C, 63.49; H, 7.02; N, 6.11%.

(d) *Ar* = 2,4,6-Me₃C₆H₂ **Cr4**. Based on the procedure described for **Cr1** but using **L4/L4'** (0.263 g, 0.60 mmol) and CrCl₃(THF)₃ (0.188 g, 0.50 mmol), **Cr4** was isolated as a brown powder (0.244 g, 82%). FT-IR (cm⁻¹): 2919 (s), 2563 (m), 2323 (m), 1699 (w), 1617 (m, ν_{C=N}), 1562 (s), 1517 (s), 1482 (vs), 1373 (s), 1263 (m), 1208 (m), 1133 (m), 1031 (w), 931 (w), 854 (s), 813 (vs). Anal. Calcd for C₃₀H₃₅N₃Cl₃Cr (595.98): C, 60.46; H, 5.92; N, 7.05%. Found: C, 60.20; H, 6.01; N, 6.89%.

(e) *Ar* = 2,6-Et₂-4-MeC₆H₂ **Cr5**. Based on the procedure described for **Cr1** but using **L5/L5'** (0.296 g, 0.60 mmol) and CrCl₃(THF)₃ (0.188 g, 0.50 mmol), **Cr5** was isolated as a brown powder (0.254 g, 78%). FT-IR (cm⁻¹): 2962 (s), 2928 (s), 2873 (s), 1612 (m, ν_{C=N}), 1588 (s), 1561 (s), 1516 (s), 1456 (m), 1372 (s), 1262 (m), 1205 (m), 1044 (w), 857 (s), 823 (vs). Anal. Calcd for C₃₄H₄₃N₃Cl₃Cr (652.09): C, 62.63; H, 6.65; N, 6.44%. Found: C, 62.38; H, 6.84; N, 6.37%.

Synthesis of epoxy-terminated polyethylene (e-PE)

A Schlenk flask containing 2.0 g of low molecular weight polyethylene [generated using **Cr2**/MAO (entry 11 Table 3)] in toluene (30 mL) was stirred for 10 min at 75 °C to form a visually clear suspension. *m*-Chloroperbenzoic acid (1.50 g, 8.67 mmol) was then introduced under nitrogen and the mixture stirred at 75 °C for 3 h. On cooling to room temperature, methanol was added to induce precipitation. The precipitate was filtered, washed with methanol and dried under reduced pressure to give e-PE as a white solid (1.42 g,

97%).^{9d} ¹H NMR (CDCl₃, 300 MHz, TMS): δ 2.90 (s, 1H), 2.74 (s, 1H), 2.46 (s, 1H), 1.35 (s, 132H), 0.97 (s, 3H). ¹³C NMR (CDCl₃, 75 MHz, TMS): δ 52.52, 47.10, 32.75, 32.24, 30.00, 26.19, 22.94, 14.27.

Crystallographic Studies

Single crystals of **Cr2** suitable for the X-ray diffraction study were grown by slow diffusion of heptane into a

Table 5 Crystal data and structure refinement for Cr2

Empirical formula	C ₃₂ H ₃₉ Cl ₃ CrN ₃
Formula weight	624.01
Temperature/ K	173.1500
Wavelength/ Å	0.71075
Crystal system	orthorhombic
space group	P2 ₁ 2 ₁ 2 ₁
<i>a</i> /Å	12.413 (3)
<i>b</i> /Å	15.526 (3)
<i>c</i> /Å	15.772 (3)
Alpha/°	90.00
Beta/°	90.00
Gamma/°	90.00
Volume/Å ³	3039.5(11)
<i>Z</i>	4
<i>D</i> _{calcd} / (g cm ⁻³)	1.364
<i>μ</i> /mm ⁻¹	0.667
<i>F</i> (000)	1308.0
Crystal size /mm	0.553 × 0.229 × 0.041
2θ range /°	3.682 to 54.976
Limiting indices	-16 ≤ <i>h</i> ≤ 16, -20 ≤ <i>k</i> ≤ 14, -20 ≤ <i>l</i> ≤ 18
No. of rflns collected	20814
No. unique rflns [<i>R</i> (int)]	6922 [<i>R</i> _{int} = 0.0344, <i>R</i> _{sigma} = 0.0326]
Completeness to θ	99.0 %
Data/restraints/parameters	6922/0/357
Goodness of fit on <i>F</i> ²	1.072
Final <i>R</i> indices [<i>I</i> > 2σ(<i>I</i>)]	<i>R</i> ₁ = 0.0430, <i>wR</i> ₂ = 0.1125
<i>R</i> indices (all data)	<i>R</i> ₁ = 0.0453, <i>wR</i> ₂ = 0.1256
Largest diff. peak and hole (e Å ⁻³)	0.46/-0.44

dichloromethane solution of the complex at room temperature. The X-ray study was carried out on a Rigaku Saturn724 + CCD with graphite-monochromatic Mo-Kα radiation (λ = 0.71073 Å) at 173(2) K; cell parameters were obtained by global refinement of the positions of all collected reflections. Intensities were corrected for Lorentz and polarization effects and empirical absorption. The structures were solved by direct methods and refined by full-matrix least squares on *F*². All hydrogen atoms were placed in calculated positions. Structure solution and refinement were performed by using SHELXT (Sheldrick, 2015).¹⁴ Details of the X-ray structure determinations and refinements are provided in Table 5.

Ethylene Polymerization

(a) *At 1 atm C₂H₄*. The polymerization at 1 atm C₂H₄ was carried out in a Schlenk tube. Under an ethylene atmosphere (1 atm), **Cr2** (1.80 mg, 3.0 μmol) was added to the Schlenk vessel, equipped with stir bar, followed by freshly distilled toluene (30 mL) and the required amount of co-catalyst. The reaction mixture was then stirred under 1 atm C₂H₄ at the pre-

determined temperature (70 °C for Cr2/MMAO, 80 °C for Cr2/MAO). After 30 min, the pressure was vented and the reaction quenched with 10% hydrochloric acid in ethanol. The polymer was washed with ethanol, then dried under reduced pressure at 50 °C and weighed.

(b) At 5/10 atm C₂H₄. The higher pressure polymerization runs were carried out in stainless steel autoclave (0.25 L) equipped with an ethylene pressure control system, a mechanical stirrer and a temperature controller. The autoclave was evacuated and backfilled with ethylene three times. When the required temperature was reached, the precatalyst (3 μmol) was dissolved in toluene (50 mL) in a Schlenk tube and injected into the autoclave containing ethylene (ca. 1 atm) followed by the addition of more toluene (30 mL). The required amount of co-catalyst and additional toluene were successively added by syringe taking the total volume to 100 mL. The autoclave was immediately pressurized to the pre-determined ethylene pressure and the stirring commenced. After the required reaction time, the reactor was cooled with a water bath and the ethylene pressure vented. Following quenching of the reaction with 10% hydrochloric acid in ethanol, the polymer was collected and washed with ethanol and dried under reduced pressure at 50 °C and weighed.

Acknowledgements

GAS thanks the Chinese Academy of Sciences for a President's International Fellowship for Visiting Scientists.

Notes and references

- (a) B. L. Small, M. Brookhart and A. M. A. Bennett, *J. Am. Chem. Soc.*, 1998, **120**, 4049; (b) G. J. P. Britovsek, V. C. Gibson, B. S. Kimberley, P. J. Maddox, S. J. McTavish, G. A. Solan, A. J. P. White and D. J. Williams, *Chem. Commun.*, 1998, 849; (c) V. C. Gibson, C. Redshaw and G. A. Solan, *Chem. Rev.*, 2007, **107**, 1745; (d) V. C. Gibson and G. A. Solan, *Top. Organomet. Chem.*, 2009, **26**, 107; (e) V. C. Gibson and G. A. Solan, in *Catalysis without Precious Metals* (Ed. R. M. Bullock), Wiley-VCH, Weinheim, 2010, 111; (f) B. L. Small, *Acc. Chem. Res.*, 2015, **48**, 2599; (g) Z. Flisak and W.-H. Sun, *ACS Catal.*, 2015, **5**, 4713; (h) W. Zhang, W.-H. Sun and C. Redshaw, *Dalton Trans.*, 2013, **42**, 8988; (i) H. Suo, G. A. Solan, Y. Ma, W.-H. Sun, *Coord. Chem. Rev.*, 2018, **372**, 101.
- (a) M. A. Esteruelas, A. M. López, L. Méndez, M. Oliván and E. Oñate, *Organometallics*, 2003, **22**, 395; (b) B. L. Small, M. J. Carney, D. M. Holman, C. E. O'Rourke and J. A. Halfen, *Macromolecules*, 2004, **37**, 4375; (c) Y. Nakayama, K. Sogo, H. Yasuda, T. Shiono, *J. Polym. Sci., Part A: Polym. Chem.*, 2005, **43**, 3368; (d) N. V. Semikolenova, V. A. Zakharov, L. G. Echevskaia, M. A. Matsko, K. P. Bryliakov, E. P. Talsi, *Catal. Today*, 2009, **144**, 334; (e) I. Vidyaratne, J. Scott, S. Gambarotta, and P. H. M. Budzelaar, *Inorg. Chem.*, 2007, **46**, 7040; (f) I. Vidyaratne, J. Scott, S. Gambarotta, and R. Duchateau, *Organometallics*, 2007, **26**, 3201.
- (a) A. Bollmann, K. Blann, J. T. Dixon, F. M. Hess, E. Killian, H. Maumela, D. S. McGuinness, D. H. Morgan, A. Neveling, S. Otto, M. Overett, A. M. Z. Slawin, P. Wasserscheid and S. Kuhlmann, *J. Am. Chem. Soc.*, 2004, **126**, 14712; (b) J. T. Dixon, M. J. Green, F. M. Hess, D. H. Morgan, *J. Organomet. Chem.*, 2004, **689**, 3641; (c) D. S. McGuinness, *Chem. Rev.*, 2011, **111**, 2321; (d) T. Agapie, *Coord. Chem. Rev.*, 2011, **255**, 861; (e) K. P. Bryliakov, E. P. Talsi, *Coord. Chem. Rev.*, 2012, **256**, 2994; (f) V. Katla, S. Du, C. Redshaw, W.-H. Sun, *Rev. Catal.*, 2014, **1**, 1; (g) S. J. Martin, T. M. Pettijohn, W. K. Reagen, Phillips petroleum CO (PHIP-C), US5331070-A, 1994; (h) S. J. Martin, W. K. Reagen, T. M. Pettijohn, Phillips petroleum CO (PHIP-C), US5393719-A, 1995.
- (a) V. K. Appukkuttan, Y. Liu, B. C. Son, C. Ha, H. Suh and I. Kim, *Organometallics*, 2011, **30**, 2285; (b) W. Zhang, W. Chai, W.-H. Sun, X. Hu, C. Redshaw and X. Hao, *Organometallics*, 2012, **31**, 5039; (c) W.-H. Sun, S. Kong, W. Chai, T. Shiono, C. Redshaw, X. Hu, C. Guo, X. Hao, *Appl. Catal., A*, 2012, **447–448**, 67; (d) J. Ba, S. Du, E. Yue, X. Hu, Z. Flisak and W.-H. Sun, *RSC Adv.*, 2015, **5**, 32720; (e) F. Huang, Q. Xing, T. Liang, Z. Flisak, B. Ye, X. Hu, W. Yang and W.-H. Sun, *Dalton Trans.*, 2014, **43**, 16818; (f) F. Huang, W. Zhang, E. Yue, T. Liang, X. Hu and W.-H. Sun, *Dalton Trans.*, 2016, **45**, 657; (g) Y. Zhang, H. Suo, F. Huang, T. Liang, X. Hu and W.-H. Sun, *J. Polym. Sci., Part A: Polym. Chem.*, 2017, **55**, 830; (h) S. Du, W. Zhang, E. Yue, F. Huang, T. Liang and W.-H. Sun, *Eur. J. Inorg. Chem.*, 2016, 1748; (i) S. Du, X. Wang, W. Zhang, Z. Flisak, Y. Sun and W.-H. Sun, *Polym. Chem.*, 2016, **7**, 4188; (j) Z. Wang, G. A. Solan, Q. Mahmood, Q. Liu, Y. Ma, X. Hao and W.-H. Sun, *Organometallics*, 2018, **37**, 380; (k) Z. Wang, G. A. Solan, W. Zhang and W.-H. Sun, *Coord. Chem. Rev.*, 2018, **363**, 92; (l) H. Suo, I. I. Oleynik, C. Bariashir, I. V. Oleynik, Z. Wang, G. A. Solan, Y. Ma, T. Liang, W.-H. Sun, *Polymer*, 2018, **149**, 45.
- (a) C. Huang, S. Du, G. A. Solan, Y. Sun and W.-H. Sun, *Dalton Trans.*, 2017, **46**, 6948; (b) Y. Zhang, C. Huang, X. Hao, X. Hu and W.-H. Sun, *RSC Adv.*, 2016, **6**, 91401; (c) C. Huang, Y. Zhang, G. A. Solan, Y. Ma, X. Hu, Y. Sun and W.-H. Sun, *Eur. J. Inorg. Chem.*, 2017, 4158.
- (a) M. Zhang, K. Wang and W.-H. Sun, *Dalton Trans.*, 2009, 6354; (b) S. Zhang, S. Jie, Q. Shi, W.-H. Sun, *J. Mol. Catal. A: Chem.*, 2007, **276**, 174; (c) A. A. Saliu, A. Maliha, M. Zhang, G. Li and W.-H. Sun, *Aust. J. Chem.*, 2008, **61**, 397; (d) R. Gao, T. Liang, F. Wang, W.-H. Sun, *J. Organomet. Chem.*, 2009, **694**, 3701.
- (a) G. B. Galland, R. Quijada, R. Rolas, G. Bazan and Z. J. A. Komon, *Macromolecules*, 2002, **35**, 339; (b) W.-H. Sun, X. Tang, T. Gao, B. Wu, W. Zhang and H. Ma, *Organometallics*, 2004, **23**, 5037.
- W. Zhang, W.-H. Sun, S. Zhang, J. Hou, K. Wedeking, S. Schultz, R. Fröhlich and H. Song, *Organometallics*, 2006, **25**, 1961.
- (a) T. C. M. Chung, *Macromolecules*, 2013, **46**, 6671; (b) F. A. Leibfarth, Y. Schneider, N. A. Lynd, A. Schultz, B. Moon, E. J. Kramer, G. C. Bazan and C. J. K. Hawker, *J. Am. Chem. Soc.*, 2010, **132**, 14706; (c) Y. Kondo, D. García-Cuadrado, J. F. Hartwig, N. K. Boen, N. L. Wagner and M. A. Hillmyer, *J. Am. Chem. Soc.*, 2002, **124**, 1164; (d) Y. Zhang, H. Li, J.-Y. Dong and Y. Hu, *Polym. Chem.*, 2014, **5**, 105; (e) H. Zhou, S. Wang, H. Huang, Z. Li, C. M. Plummer, S. Wang, W.-H. Sun and Y. Chen, *Macromolecules*, 2017, **50**, 3510.
- (a) Y. Inoue, K. Matyjaszewski, *J. Polym. Sci., Part A: Polym. Chem.*, 2004, **42**, 496; (b) A. V. Sessa Sainath, M. Isokawa, M. Suzuki, S. Ishii, S. Matsuura, N. Nagai and T. Fujita, *Macromolecules*, 2009, **42**, 4356; (c) K. Matoishi, K. Nakai, N. Nagai, H. Terao, T. Fujita, *Catal. Today*, 2011, **164**, 2; (d) A. M. Anderson-Wile and G. W. Coates, *Macromolecules*, 2012, **45**, 7863; (e) J. Mazzolini, O. Boyron, V. Monteil, D. Gignes, D. Bertin, F. D'Agosto and C. Boisson, *Macromolecules*, 2011, **44**, 3381.
- N. N. Schwartz and J. H. Blumbergs, *J. Org. Chem.*, 1964, **29**, 1976.
- (a) D. Tanner and T. Groth, *Tetrahedron*, 1997, **53**, 16139; (b) G. Sabitha, R. S. Babu, M. Rajkumar, C. S. Reddy and J. S. Yadav, *Tetrahedron Lett.*, 2001, **42**, 3955; (c) B. Das, V. S.

- Reddy, M. Krishnaiah, Y. K. Rao, *J. Mol. Catal. A: Chem.*, 2007, **270**, 89; (d) A. Bukowska and W. Bukowski, *Org. Process Res. Dev.*, 2002, **6**, 234.
- 13 P. Boudjouk and S. Jeung-Ho, *Inorg. Synth.* 1992, **29**, 108.
- 14 (a) G. M. Sheldrick, *Acta Crystallogr., Sect A: Found. Adv.*, 2015, **71**, 3; (b) G. M. Sheldrick, *Acta Crystallogr., Sect C: Struct. Chem.*, 2015, **71**, 3.